9. Discussion

9.1. Measurement precisions

In the iceGGO and NOAA-ICP experiments, all participating laboratories reported measurement precisions, although their estimation methods differed. Figure 12 shows frequency distributions of the measurement precisions reported by all participating laboratories in Japan for CO_2 with NDIR, CH_4 with GC/FID, CO with GC/RGD and VURF, and N_2O with GC/ECD.

The CO_2 analyses with NDIRs were very precise. The precisions were less than 0.045 ppm for all of the laboratories, although different types of NDIRs were used. The mean of all reported precisions for the CO_2 measurements was 0.014 ppm (n = 104). Most of the CH_4 measurement errors were less than 2 ppb, although several precisions greater than 3.5 ppb were derived from the extrapolated calibrations of the JMA. The mean of all reported precisions for the CH_4 measurements was 1.4 ppb (n = 84), which was similar to the overall precision of less than 1.5 ppb for the NOAA study, which involved use of a GC/FID (Dlugokencky et al., 2005). The CO measurement precisions for the GC/RGD and VURF methods were less than 1 ppb, but the precision of the GC/FID method used by the MRI was larger. All reported precisions for the CO measurements were high, the mean being 0.37 ppb (n = 34). The precision for the GC/FID method was especially large. Most of the N_2O measurement precisions with the GC/ECD method used by the NIES and TU were less than 0.3 ppb, but larger precisions were often observed for the JMA measurements. The mean of all reported errors for the N_2O measurements made by these three laboratories was 0.31 ppb (n = 42).

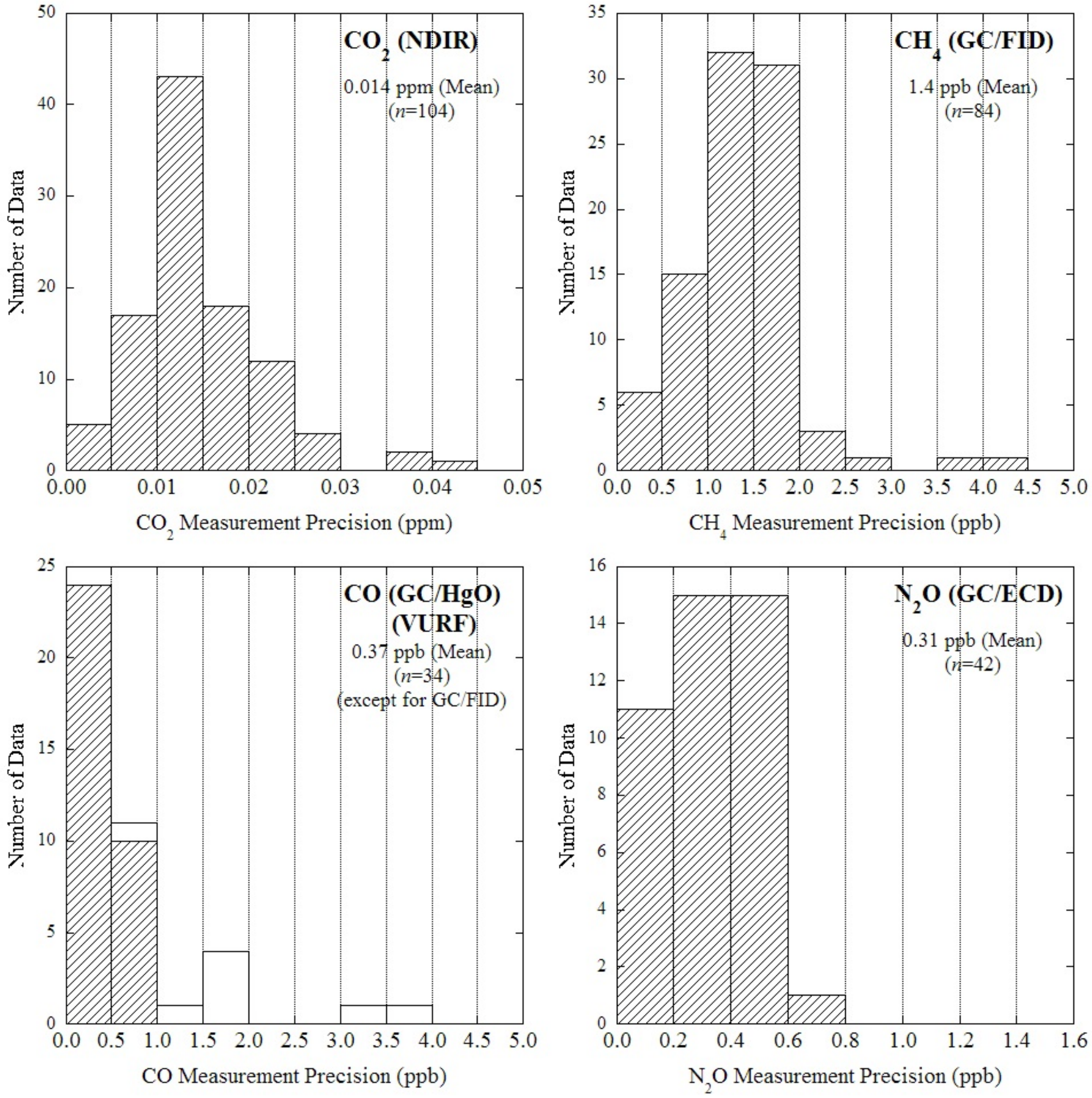

Figure 12. Frequency distributions of measurement precisions reported by all participating laboratories for CO_2, CH_4, CO, and N_2O. Open bars in the case of CO represent the precisions of the GC/FID measurements.

9.2. CH_4 scale adjustment

CH_4 comparative data were collected from three experiments, iceGGO-1, iceGGO-6, and NOAA-ICP, to address differences of CH_4 standard gas scales. These experiments revealed a difference of ~ 12 ppb in the CH_4 concentrations measured by the participating laboratories. It was clearly apparent that the differences of the CH_4 concentrations from the JMA values (Laboratory X minus JMA) increase with an increase of the concentrations for all the other laboratories (Figure 13).

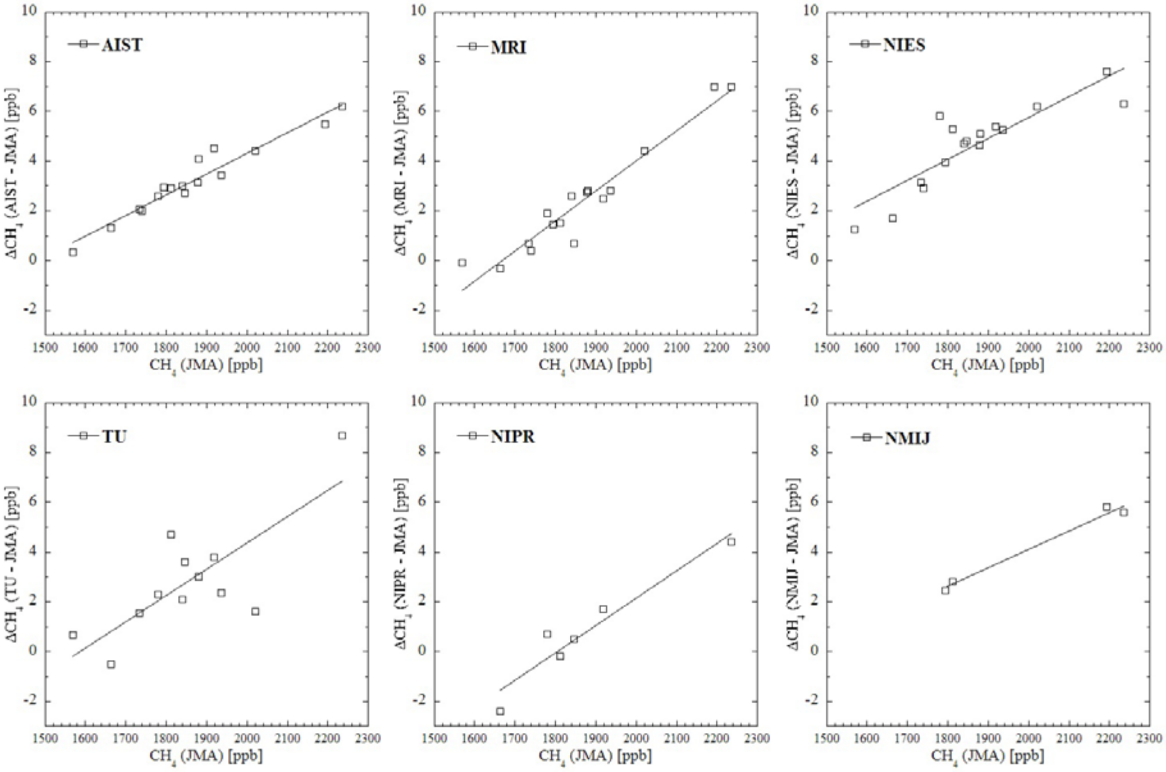

Figure 13. Differences of the measured CH_4 concentrations between participating laboratory and the JMA values as a function of CH_4 concentrations for the AIST, MRI, NIES, TU, NIPR, and NMIJ. The solid line represents the least-squares fit to all data points from three experiments: iceGGO-1, iceGGO-6, and NOAA-ICP.

The differences were therefore fitted with a linear regression line to examine their empirical relationship as follows:

$$C_X - C_{JMA} = a + b(C_{JMA}), \qquad (3)$$

where C_X and C_{JMA} are the measured CH_4 concentrations of Laboratory X and JMA, respectively. Table 31 lists the coefficients from the best fits of Eq. (3) for the six laboratories. These linear relationships clearly revealed that the differences of the CH_4 concentrations, which ranged from about 1550 to 2250 ppb, were well described by a straight line. The correlation coefficients (*r*) exceeded 0.78 (Table 31). These results indicate that all measured CH_4 concentrations from the six laboratories could be re-calculated with a simple linear relationship to adjust the values to the same standard gas scale.

Table 31. Coefficients obtained with linear least square fits of Eq. (3) to the differences of the CH_4 concentrations from the JMA values for the six laboratories.

Laboratory	*a*	*b*	*r*
AIST	-12.3	0.00833	0.97
MRI	-20.3	0.01215	0.96
NIES	-11.1	0.00846	0.87
TU	-16.8	0.01059	0.78
NIPR	-19.9	0.01102	0.96
NMIJ	-10.8	0.00744	0.99

Figure 14 shows a frequency distribution of the differences of all CH_4 concentrations (n = 70) from the JMA values for the three intercomparison experiments. The differences were widely distributed from –3 ppb to 9 ppb, and they often exceeded the criterion for compatibility of CH_4 measurements (± 2 ppb) recommended by the WMO. This result strongly reflects differences in the CH_4 standard gas scales among the participating laboratories. These differences were therefore re-calculated based on the linear fit of Eq. (3) using the coefficients in Table 31, and their frequencies are shown in Figure 14. After a scale adjustment, the frequency distribution of the re-calculated differences covered a relatively narrow range, from –2 ppb to +2 ppb with a mean near zero, with the caveat that two data points deviated from this range. This result indicates that the re-calculation of fits from our comparison experiments was suitable for making datasets consistent by adjusting for differences of the standard gas scales by all participating laboratories.

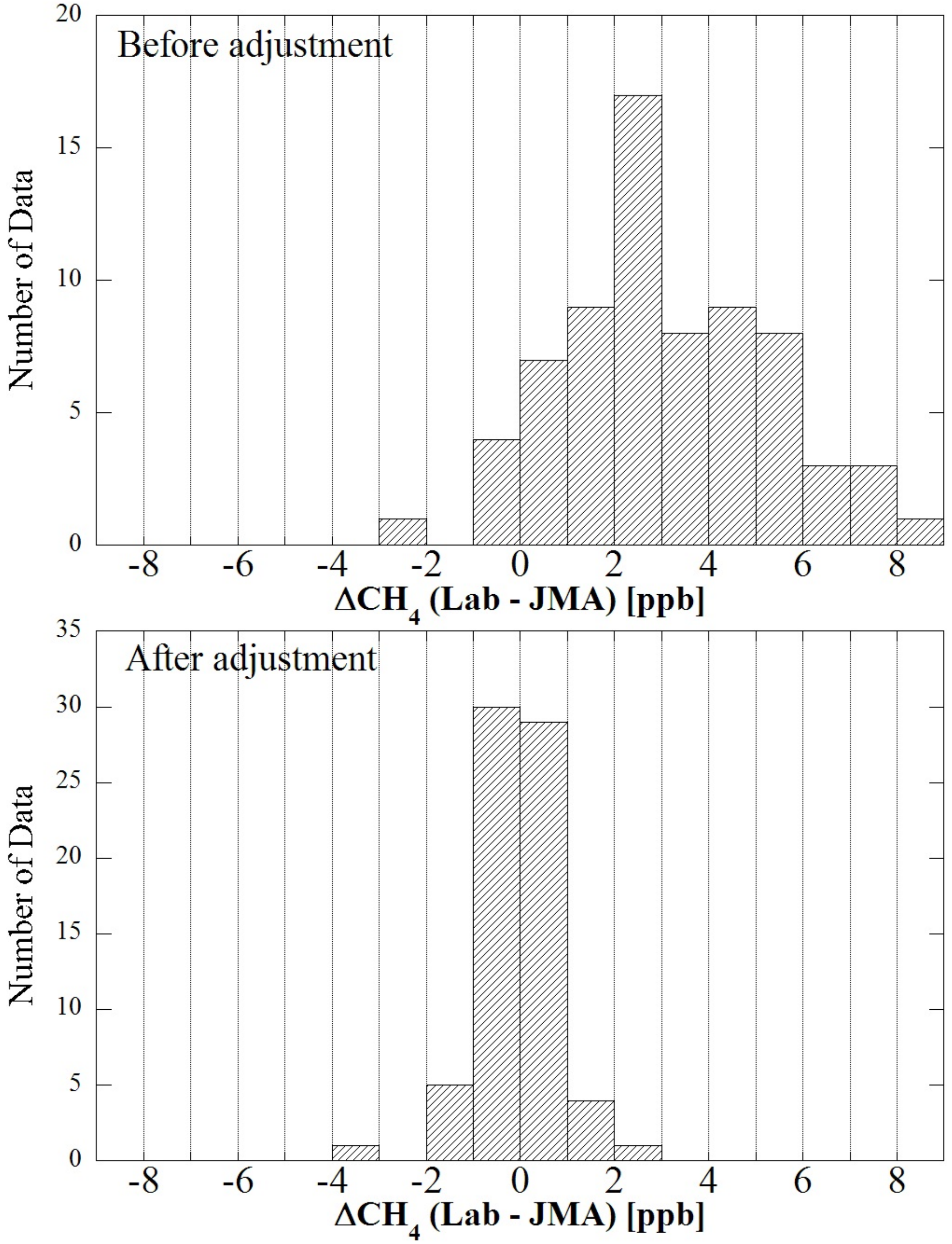

Figure 14. Frequency distributions of differences of all CH_4 measurements (n = 70) from the JMA for the three intercomparison experiments before and after scale adjustments.

9.3. CO scale adjustment

The CO comparison data were collected from two experiments, iceGGO-4 and NOAA-ICP, to focus on the difference of CO standard gas scales. For the iceGGO-4, CO concentrations in the two cylinders were found to increase with time during the experimental period of about one year. These CO increases were described rather well by linear regressions based on the three NIES measurements (Figure 15). The linear drift of CO concentrations was estimated to be about +3.2 ppb/yr for the CPB28680 cylinder and +4.7 ppb/yr for the CPB16249 cylinder. A similar CO concentration increase was also found in all six cylinders during the NOAA-ICP experiment when the measurements of the NOAA and Empa at the beginning and the end of the experiment were compared (Figure 8). The average linear drift of the CO concentrations for the NOAA-ICP experiment was estimated to be about 1 ppb/yr, which was smaller than the drift for the iceGGO-4 experiment, probably due to the difference of cylinder volume.

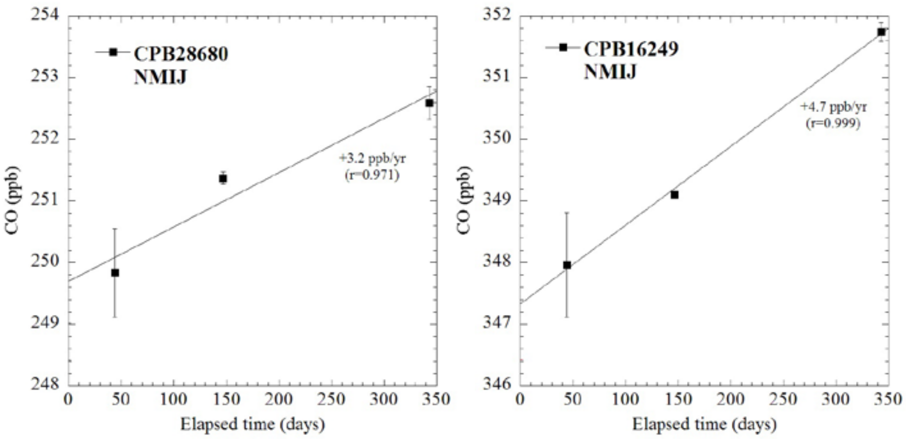

Figure 15. Changes of CO concentrations in the two cylinders (CPB28680 and CPB16249) with elapsed time during the iceGGO-4 experiment. The slopes of the linear regression lines represent CO drifts of +3.2 ppb/yr and +4.7 ppb/yr.

All reported CO values were therefore corrected based on the estimated drifts as stated above, and they were then compared to calculate the differences of CO concentrations among the participating laboratories. These results revealed a difference of ~16 ppb for the corrected CO measurements among all the laboratories. It was apparent that the differences of the CO concentrations from the NIES values (Laboratory X minus NIES) were rather well described by a linear regression line, although the TU and NIES relationships were described by two regression lines (Figure 16).

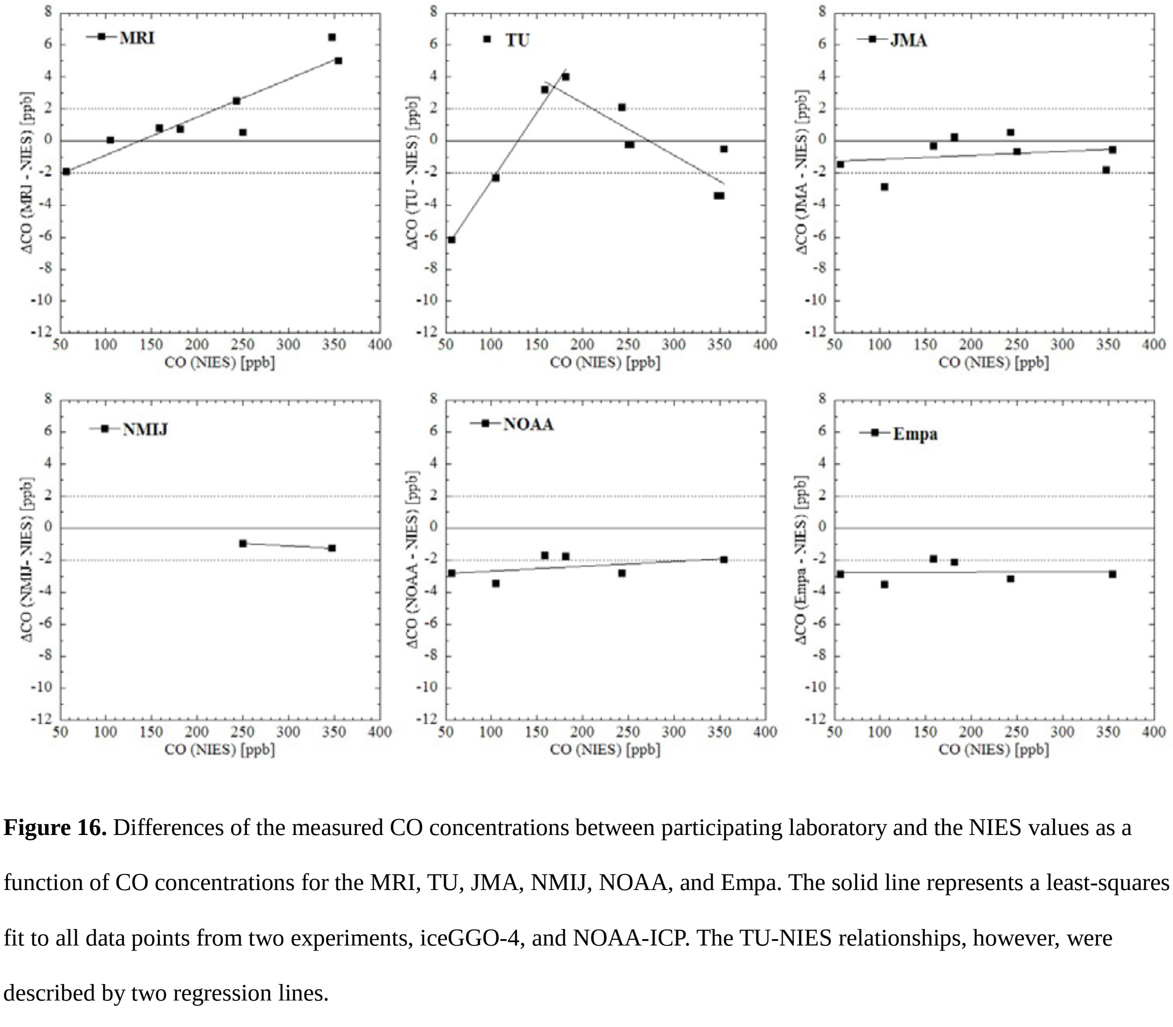

Figure 16. Differences of the measured CO concentrations between participating laboratory and the NIES values as a function of CO concentrations for the MRI, TU, JMA, NMIJ, NOAA, and Empa. The solid line represents a least-squares fit to all data points from two experiments, iceGGO-4, and NOAA-ICP. The TU-NIES relationships, however, were described by two regression lines.

The differences for each laboratory were fitted by a linear regression line to examine their empirical relationships as follows:

$$C_{\mathrm{X}} - C_{\mathrm{NIES}} = a + b(C_{\mathrm{NIES}}), \qquad (4)$$

where C_{X} and C_{NIES} are the corrected CO concentrations of Laboratory X and the NIES, respectively. Table 32 lists the coefficients from the best fits of Eq. (4) for the six laboratories. These linear relationships clearly revealed that the differences of the CO concentrations, which ranged from about 50 ppb to 350 ppb, depended on the CO concentrations. These results indicate that all of the CO measurements from the six laboratories could be re-calculated with a simple linear relationship to adjust the values to a common standard gas scale.

Table 32. Coefficients obtained by linear least-squares fits of Eq. (4) to the differences of the drift of the corrected CO concentrations from the NIES values for the six laboratories.

Laboratory	*a*	*b*	*r*	Range of CO (ppb)
MRI	-3.25	0.024	0.93	50-350
TU	-11.03	-0.086	0.99	50-170
TU	8.84	-0.032	0.90	170-350
JMA	-1.38	-0.003	0.24	50-350
NMIJ	-0.16	-0.003	1.00	250-350
NOAA	-2.95	0.003	0.45	50-350
Empa	-2.77	0.002	0.03	50-350

Figure 17 shows frequency distributions of the differences of all CO measurements (n = 38) from the NIES values for the two intercomparison experiments before and after scale adjustments. The differences before the scale adjustments were widely distributed, from –8 ppb to +8 ppb, and they often exceeded the criterion for compatibility of CO measurements (±2 ppb) recommended by the WMO. This result strongly reflects differences in the reference CO standard gas scales among the participating laboratories. The differences were therefore re-calculated based on the linear fit of Eq. (4) using the coefficients in Table 32, and their frequency distribution is shown in Figure 17. The frequency distribution after the scale adjustment was narrower, the range of differences being –2 ppb to +2 ppb with a mean near zero, with the caveat that several data points deviated from this range. This result indicates that the re-calculated fits from our comparison experiments are suitable for making consistent datasets from the observed CO concentrations from all the laboratories by adjusting the difference of the CO standard scales.

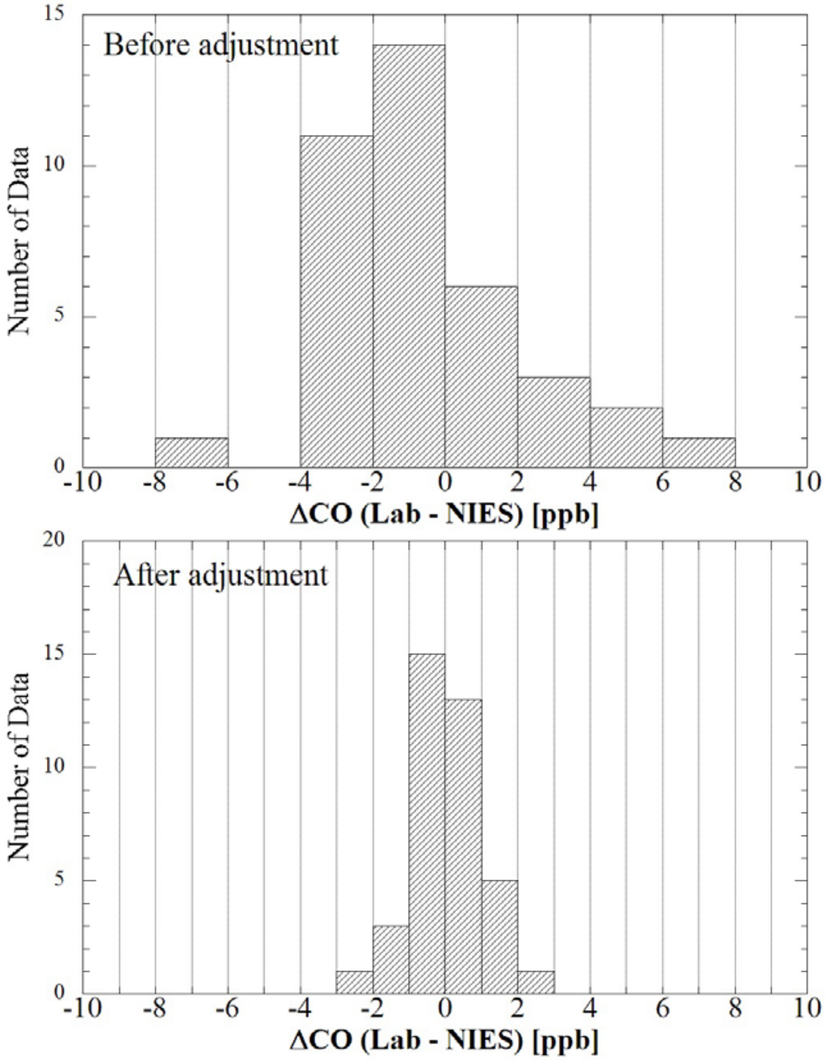

Figure 17. Frequency distributions of the differences of all the CO measurements (n = 38) from the NIES values for the two intercomparison experiments before and after scale adjustments.

9.4. CO_2 scale adjustment

The CO_2 measurement biases from the NIES values, estimated from Figure 18 using the results of the iceGGO-2 experiment, were 0.21 ppm for the TU, 0.16 ppm for the AIST, and 0.25 ppm for the NIPR. In contrast, the difference between the JMA and NIES values clearly decreased with increasing CO_2 concentration. The relationship could be fitted according to the linear equation $C_{\mathrm{JMA}} - C_{\mathrm{NIES}} = 0.867 + 0.0020602(C_{\mathrm{JMA}})$, where C_{JMA} and C_{NIES} are the CO_2 concentrations measured by the JMA and NIES, respectively.

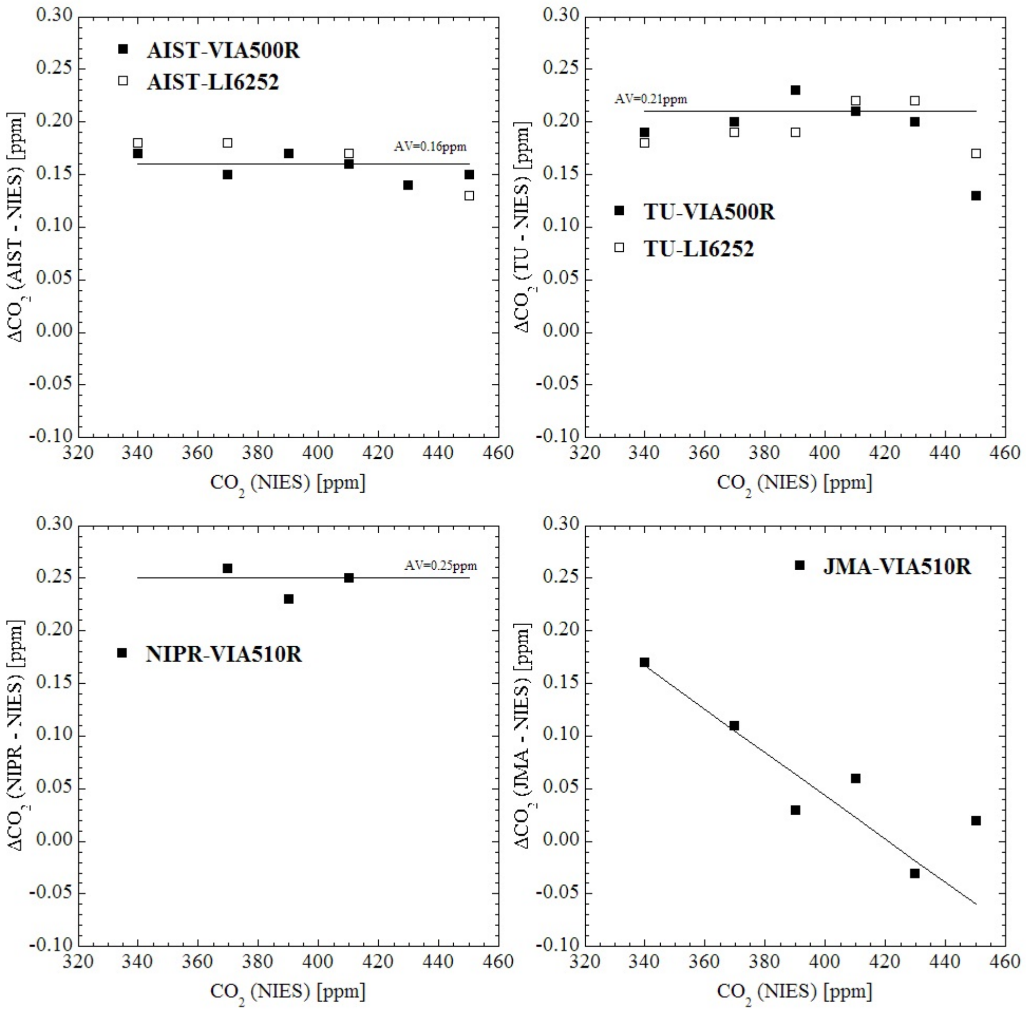

Figure 18. Differences of the measured CO_2 concentrations between participating laboratories and the NIES values as a function of CO_2 concentrations for the AIST, TU, NIPR, and JMA. The AIST and TU used two different analyzers. The solid line represents the estimated scale bias based on all data points from the iceGGO-2 experiment, which was based on six round-robin cylinders with isotopically lighter CO_2 derived from combusted petroleum.

Taking into consideration these estimated biases, the differences from the NIES values were re-calculated, and the values were then compared before and after the scale adjustment (Figure 19). The large deviations of the differences among the laboratories were significantly reduced after re-calculation, and the averaged differences were smaller. It was apparent that most of the CO_2 measurements from all six laboratories could be adjusted to within ±0.02 ppm based on the measurement scale biases from the iceGGO-2 experiment.

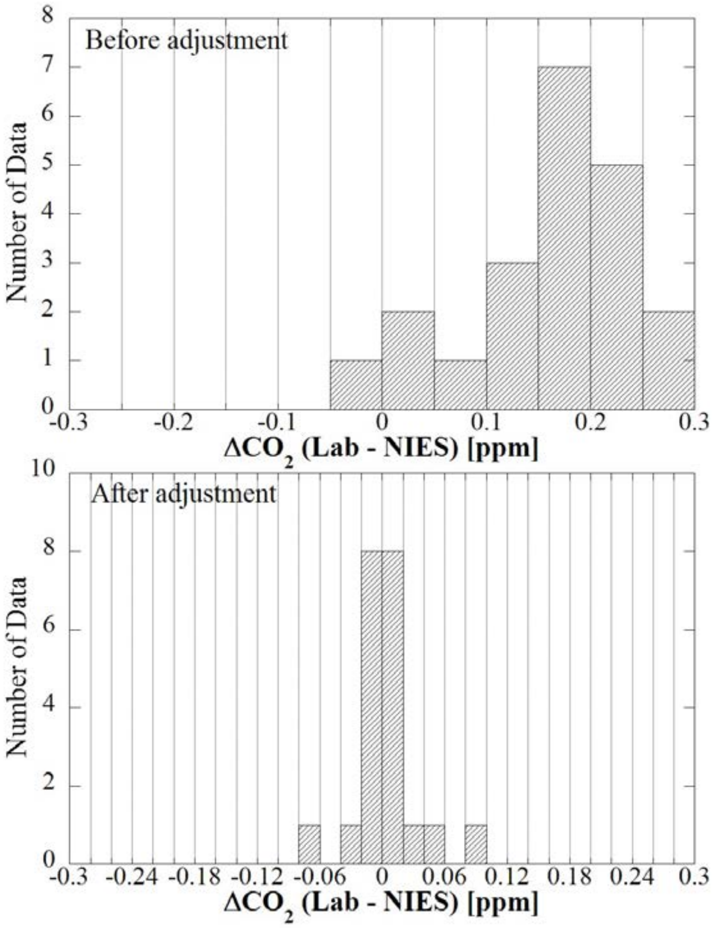

Figure 19. Frequency distributions of differences of all CO_2 measurements (n = 21) from the NIES values for the iceGGO-2 experiment before and after scale adjustments.

9.5. CO_2 isotope effect

In general, the NDIR analyzers used for the CO_2 measurements have mechanisms to reduce the interference effects from other infrared-active species. In the case of the LI-COR NDIR analyzers, including the LI-6252, optical bandpass filters designed to transmit wavelengths for a fundamental absorption band of $^{12}C^{16}O_2$ are placed between the sample cell and the detector to enhance the selective sensitivity to the CO_2. Unfortunately, the bandpass filter blocks a substantial part of the absorption band of $^{13}C^{16}O_2$, because the absorption region for $^{13}C^{16}O_2$ in substantial part overlaps those of N_2O and CO. Therefore, the LI-COR NDIR analyzer has different relative molar sensitivities to the different CO_2 isotopologues ($^{12}C^{16}O_2$, $^{13}C^{16}O_2$, $^{12}C^{18}O^{16}O$, etc) that could potentially result in different responses to CO_2-in-air samples with the same bulk CO_2 mixing ratio but different isotopic compositions (Tohjima et al., 2009). This feature of the LI-COR NDIR analyzer resulted in significant errors in the measurement of the CO_2 mixing ratio of the ambient air sample because the CO_2 standard gases of all the laboratories participating in the iceGGO experiments were mixtures of purified natural air and isotopically light CO_2 gases derived from combusted petroleum.

In the iceGGO-2 and iceGGO-3 interlaboratory comparison experiments and the NOAA-ICP, three types of NDIR analyzers, VIA-500R, VIA-510R, and LI-6265, were used to measure the round-robin gas concentrations with a wide range of CO_2 isotopic compositions. We thus evaluated the isotope effects of the NDIR analyzers by using the results of the 12 cylinders for which the CO_2 isotopic compositions were significantly different from those of the CO_2 standard gases used in each laboratory (Table 33). The apparent differences in the measured CO_2 mixing ratios caused by the NDIR isotope effect were evaluated as follows. First, the CO_2 mixing ratios for the 12 cylinders determined by the AIST, JMA, and TU were converted to values based on the NIES CO_2 scale by using the adjustment factors described in section 9.4. Then, the differences of the adjusted CO_2 mixing ratios from the NIES values were computed (Table 33). Because the CO_2 mixing ratios determined by the LI-6252 at the NIES were precisely (within ±0.01 ppm) corrected for the isotope effect by adopting the approach of Tohjima et al. (2009), we considered these apparent differences to be due mainly to the isotope effect of the NDIR analyzers.

Table 33. Summary of CO_2 mixing ratios and isotopic values (δ^{13}C and δ^{18}O) for the 12 round-robin cylinders used to evaluate the isotope effect of the five NDIR analyzers[a].

Cylinder #	$CO_{2,NIES}$	δ^{13}C[c]	δ^{18}O[c]	$CO_{2,X}$-$CO_{2,NIES}$[b]				
	NIES(6252)	‰,VPDB		AIST(6252)	AIST(500R)	JMA(510R)	TU(500R)	TU(6252)
iceGGO-2								
CPB28548	370.06(2)	57.3	-28.4	-0.29(2)	-0.05(2)	-0.18(2)	-0.01(2)	-0.34(2)
CPB16443	406.02(1)	-8.8	0.4[d]	-0.14(2)	-0.02(2)	-0.06(2)	-0.01(2)	-0.12(3)
CPB29524	409.31(1)	-9.0	0.4[d]	-0.14(2)	-0.02(2)	-0.06(1)	0.00(1)	-0.12(2)
iceGGO-3								
CPD00070	379.55(1)	-8.9	-13.0	-	-0.03(2)	-0.04(2)	0.00(1)	-0.10(1)
CPD00076	399.18(1)	-9.0	-13.2	-	-0.01(2)	-0.08(2)	0.00(1)	-0.11(2)
CPD00069	417.78(1)	-8.9	-13.1	-	-0.02(2)	0.01(2)	-0.02(1)	-0.11(1)
NOAA-ICP								
CB09739	355.08(0)	-8.9	-24.3	-	-0.03(1)	0.00(2)	-0.05(1)	-
CB10067	376.20(1)	-8.8	-9.8	-	0.06(1)	-0.03(2)	0.04(1)	-
CB09997	389.90(1)	-8.7	-1.4	-	0.04(1)	-0.08(1)	0.05(1)	-
CB09977	397.29(0)	-8.6	-1.5	-	0.05(1)	-0.06(1)	0.06(1)	-
CB09973	404.91(1)	-8.7	-2.2	-	0.06(1)	-0.03(2)	0.08(1)	-
CB10036	419.64(0)	-8.7	-3.6	-	0.05(1)	0.02(1)	0.02(1)	-

[a] Uncertainty of the last digit is expressed by parentheses.

[b] Calculated after the CO_2 mixing ratios for the individual laboratories are adjusted to the NIES standard scale by using the adjustment factors described in section 9.4.

[c] Isotope ratios are measured by AIST except CPB28548, CPB16443, and CPB29524, which are measured by NIES.

[d] Assumed to be the same as the values for the atmospheric CO_2 given in Tohjima et al. (2009).

Figure 20 shows the apparent differences in the CO_2 mixing ratios of the 12 round-robin cylinders determined by the five NDIR analyzers. It is of interest that the apparent differences for the two VIA-500R analyzers used at TU and AIST were within ±0.1 ppm, even when the ^{13}C-enriched CO_2-in-air mixture in the CPB28548 cylinder ($\delta^{13}C$ = +57.3 ‰) was measured. This result indicates that correction for the isotope effect was unnecessary for the CO_2 measurements made with the VIA-500R analyzers. In contrast, the VAI-510R and LI-6252 analyzers clearly showed negative differences (Laboratory X – NIES) due to the isotope effect, whereas the magnitudes of the differences for the LI-6252 were twice those for the VAI-510R.

We evaluated the observed isotope effects by adopting the approach used by Tohjima et al. (2009). We assumed that the VIA-500R and VIA-510R analyzers also used the same type of bandpass filter as the LI-COR analyzer. First, a gravimetric mixture of pure $^{13}CO_2$ gas and purified natural air was measured by each NDIR analyzer. All the NDIR analyzers gave $^{13}CO_2$ mixing ratios that were substantially lower than the gravimetric values of about 380 ppm and 400 ppm (Table 34), and the apparent $^{13}CO_2$ mixing ratios were related to the overlap between the absorption band of $^{13}CO_2$ and the wavelength transmitted by the bandpass filters for the NDIR analyzers. Thus, the position of the bandpass filter in the wavenumber domain was determined from the apparent $^{13}CO_2$ mixing ratio for each NDIR analyzer.

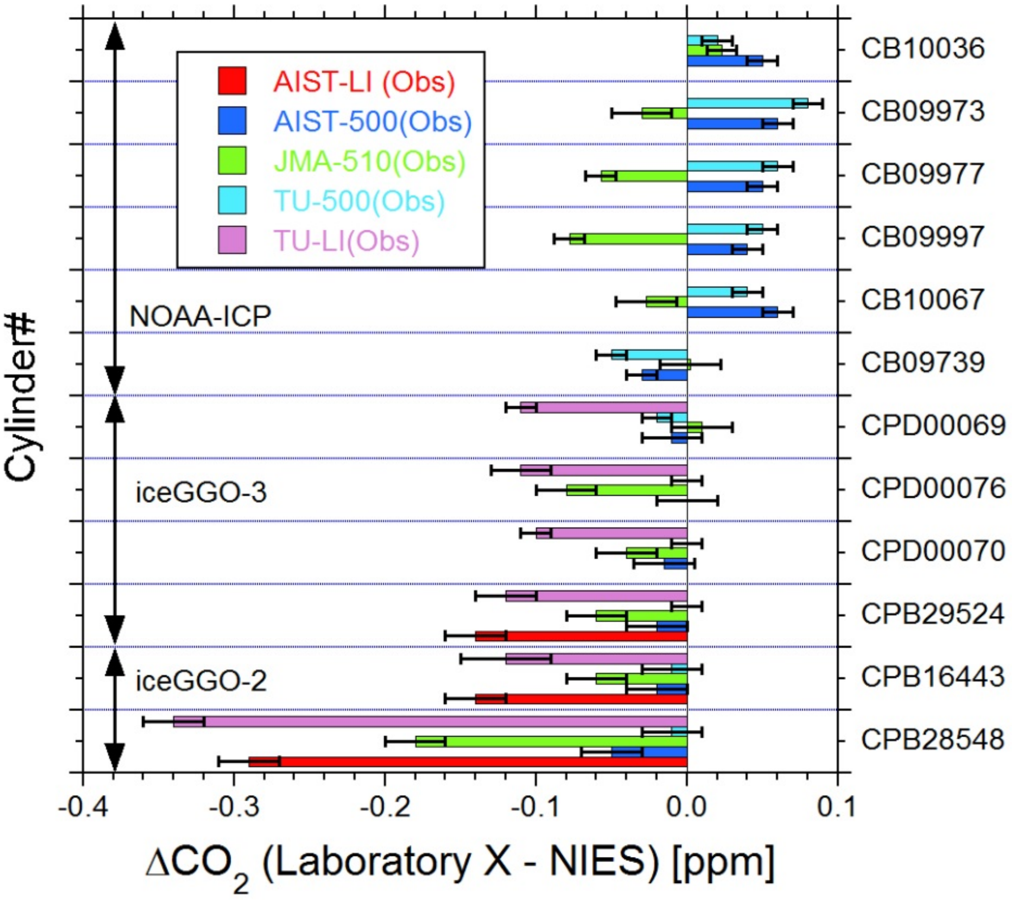

Figure 20. Differences of CO_2 mixing ratios determined by the five NDIR analyzers at the three laboratories from those determined by the LI-6252 analyzer at the NIES for the 12 round-robin cylinders. The differences in the CO_2 standard scales between the laboratories were adjusted to the NIES scale, and the CO_2 mixing ratios given by the NIES were corrected for the isotope effect of the NDIR analyzer. The plotted CO_2 differences are thus considered to reflect mainly the isotope effect of the individual NDIR analyzers.

Table 34. Apparent mixing ratios of gravimetric $^{13}CO_2$-in-air mixture determined by NDIR analyzers.

Laboratory	NDIR	NDIR Detector	Measurement date	$^{13}CO_2$ (ppm)	Measured $^{13}CO_2$ (ppm)
AIST	Beckman880	microphone condenser	2008/12/10	380.13	23.54
AIST	LI6252_IRG2-408*	semiconductor	2012/5/27	400.11	32.50
AIST	LI6262-1237	semiconductor	2008/12/2	380.13	39.41
AIST	BINOS MLT3.1	flow sensor	2008/12/9	380.13	51.97
AIST	LI6262-1333	semiconductor	2008/12/1	380.13	61.14
AIST	LI6262-452	semiconductor	2008/12/1	380.13	72.44
AIST	VIA-500R*	microphone condenser	2008/12/1	380.13	76.07
MRI	LI7000_IRG4-0768	semiconductor	2011/10/4	380.13	16.35
MRI	LI6252_IRG2-0568*	semiconductor	2011/10/4-5	380.13	30.47
MRI	LI7000_IRG4-0799	semiconductor	2011/10/5	380.13	30.56
MRI	Binos 4.1b	flow sensor	2008/2/1	380.13	67.67
MRI	VIA-510R	microphone condenser	2008/11/15	380.13	73.10
NIES	LI6252_IRG3-645	semiconductor	Tohjima et al. (2009)	380.00	27.34
NIES	LI6252_IRG2-654*	semiconductor	Tohjima et al. (2009)	380.00	45.68
NIES	LI6252_IRG2-246	semiconductor	Tohjima et al. (2009)	380.00	93.66
TU	LI6252*	semiconductor	2012/12/13	380.13	29.72
TU	VIA-500R*	microphone condenser	2012/12/13	380.13	82.59
JMA	VIA-510R*	microphone condenser	2013/05/01&06/04	380.13	50.52
JMA	LI7000_IRG4-0767	semiconductor	2013/5/1	380.13	19.97
JMA	LI7000_IRG4-0926	semiconductor	2013/6/4	380.13	24.19

*NDIR instruments used for the iceGGO experiments

Finally, we could evaluate the isotope effect of each NDIR analyzer for any CO_2-in-air mixture by taking into account the fractional abundances of CO_2 isotopologues, which are easily calculated from δ^{13}C and δ^{18}O values (Tohjima et al., 2009). The calculated apparent differences of the CO_2 mixing ratios for the round-robin cylinders for the individual NDIR analyzers are plotted in Figure 21. In the calculations we assumed that the isotopic compositions of the CO_2 standard gases used by the AIST, JMA, and TU were the same as those used by the NIES. As is apparent, the data for the LI-6252 analyzers, shown as circles and triangles in the figure, were scattered around the 1:1 line of the relationship, the indication being that the isotope effect of the LI-6252 analyzer could be rather well predicted with the approach of Tohjima et al. (2009). However, this approach cannot necessarily evaluate the isotope effects of the other NDIR analyzers satisfactorily, especially the VIA-500R.

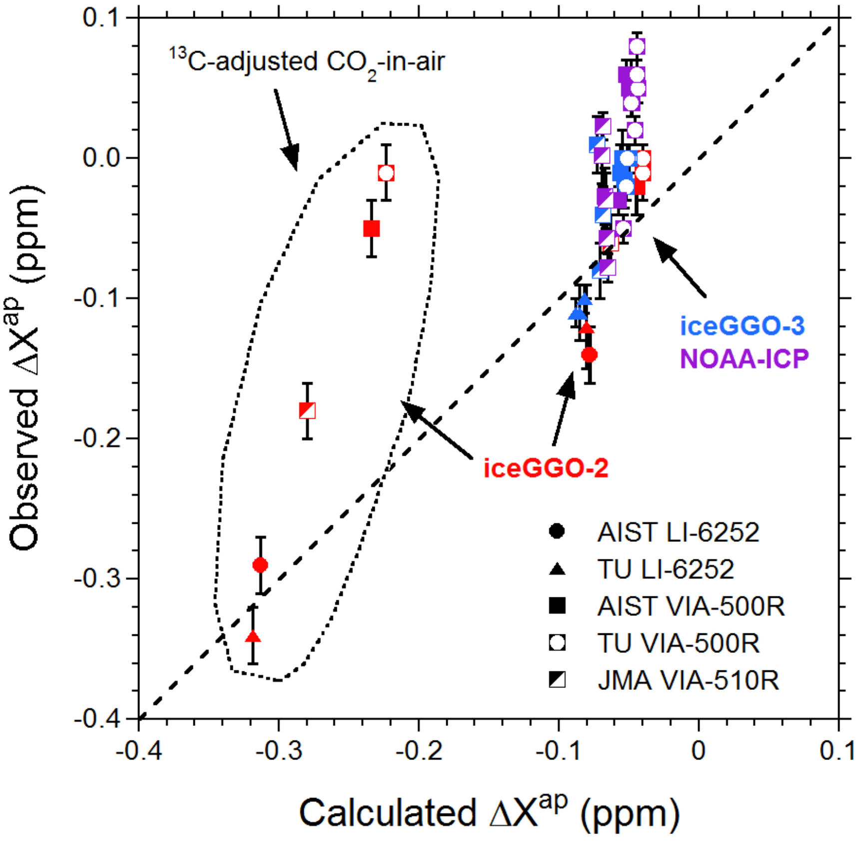

Figure 21. Relationship between the observed and calculated apparent differences in the CO_2 mixing ratios for the 12 round-robin cylinders caused by the isotope effects of the five NDIR analyzers. The observed values are the differences of the CO_2 mixing ratios determined by the AIST, TU, and JMA from those determined by the NIES (Laboratory X – NIES) after the standard scales of the three laboratories were adjusted to that of the NIES. The straight line represents the 1:1 relationship.

9.6. N_2O scale adjustment

The N_2O comparison data were collected from two experiments, iceGGO-5 and NOAA-ICP, to focus on the difference of the N_2O standard gas scales. Figure 22 shows the differences of the measured N_2O concentrations between the participating laboratories and the NIES as a function of the N_2O concentrations. The concentrations measured by the TU and AIST were higher by about 1 ppb than those measured by the NIES using the GC/ECD method. The values measured by the MRI and JMA with the ICOS were also higher than those measured by the NIES. These results indicate that all measured N_2O concentrations from the five laboratories could be re-calculated with simple linear relationships that would greatly reduce the standard scale differences. However, the reduced differences often exceeded the compatibility criterion for N_2O measurements (±0.1 ppb) recommended by the WMO because that goal is not easily achieved. The relationship between the NOAA and NIES values revealed a systematic difference between the iceGGO-5 and NOAA-ICP experiments. This difference was not observed in the relationship between the JMA and NIES concentrations measured via GC/ECD. Because the relatively large uncertainty of the GC/ECD analysis remained, further and more accurate comparisons using a high-precision mid-IR laser-based instrument will be needed to validate the differences of the N_2O standard gas scales.

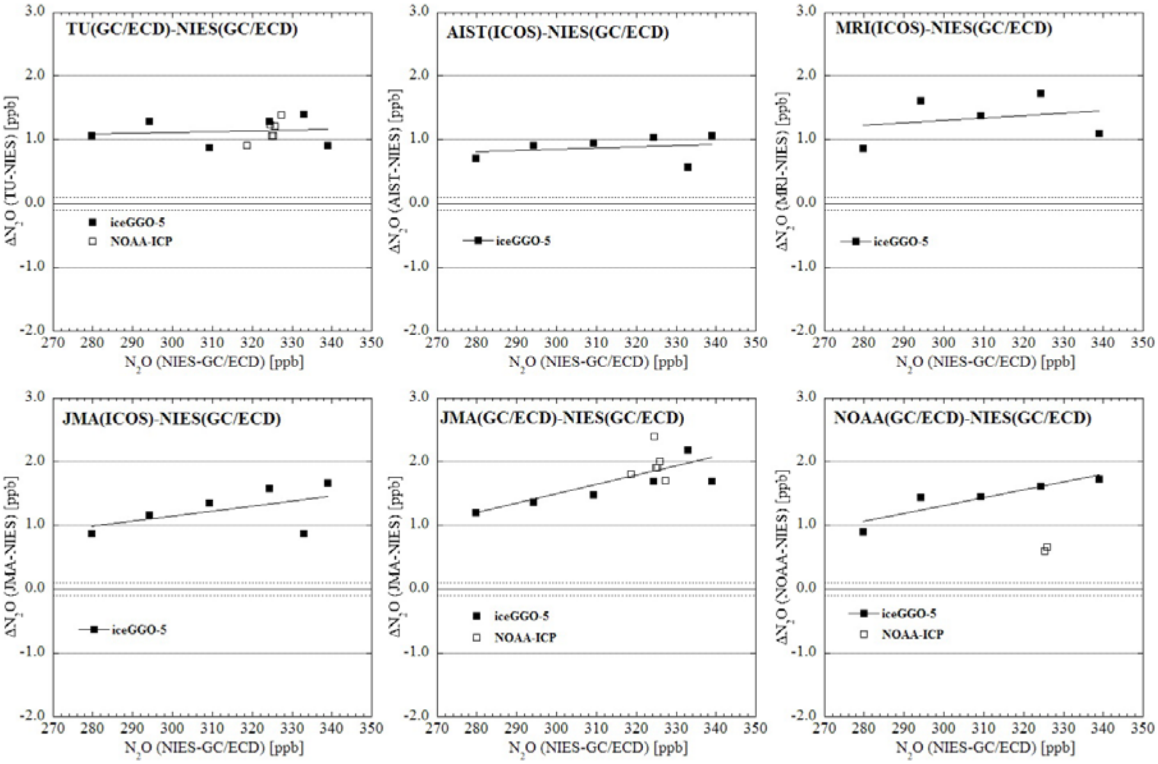

Figure 22. Differences of the measured N_2O concentration between participating laboratories and the NIES as a function of N_2O concentrations for the TU, AIST, MRI, JMA, and NOAA datasets. The solid line represents a least-squares fit to all data points from the iceGGO-5 and NOAA-ICP experiments.

Acknowledgements

We are grateful to Paul Novelli of NOAA for his collaboration with the NOAA-ICP experiment. Many support staff in the OCCCO, as well as measurement and logistic collaborators at the JMA, contributed directly to this iceGGO program. Editing of this article was supported by the Ministry of the Environment in Japan as a contribution to the Japanese Alliance for Climate Change Observation.